Magazine of Concrete Research, 2010, **62**, No. 8, August, 569–583
doi: 10.1680/macr.2010.62.8.569

Deformability evaluation of high-strength reinforced concrete columns

J. C. M. Ho and H. J. Pam

University of Hong Kong

Plastic hinge length and ultimate curvature are the crucial parameters that enable inelastic deformability (deflection and rotation) of reinforced concrete columns to be evaluated. Prediction of deformability beyond the elastic range is important in the performance-based design of earthquake-resistant structures. Although large numbers of tests have been conducted in the past by numerous researchers on reinforced concrete columns subjected to simultaneous axial load and large inelastic displacement, available design tools that enable rapid evaluation of deformability of reinforced concrete columns are still limited. The situation is even worse for high-strength reinforced concrete columns. The objective of this paper is to investigate plastic hinge length and ultimate curvature for deformability evaluation of high-strength reinforced concrete columns. In connection with this, two equations are proposed in this paper for estimating the plastic hinge length and ultimate curvature of high-strength reinforced concrete columns leading to their deformability evaluation. The proposed equations are used to evaluate the theoretical deflection of other researchers' column test specimens, and it is proven that these theoretical deflections mostly underestimate slightly their respective measured deflections. Therefore, the proposed equations can be used for conservative estimation of high-strength reinforced concrete column deformability at an early design stage without performing the tedious load–deflection analysis.

Notation

A_c	core concrete area measured to outside of confinement reinforcement
A_g	gross cross-sectional area
d_s	diameter of transverse steel (Table 1)
f'_c	specified concrete cylinder strength
f_y	specified yield strength of longitudinal reinforcement
f_{ys}	specified yield strength of confinement or transverse reinforcement
H	distance between points of contra-flexure and maximum bending moment (= 1895 mm)
H'	distance between point of contra-flexure and the point where the maximum lateral displacement is measured (= 317·5 mm)
H''	distance between point of contra-flexure and top of column flange
h	larger cross-sectional dimension of column
L_{CR}	length of critical region
ℓ_p	plastic hinge length
M_p	measured maximum moment capacity
M_u	unconfined flexural strength of column estimated according to Eurocode 2
P	compressive axial load
R	prefix for mild steel round bar with specified yield strength of 250 MPa (Table 1)
R	horizontal reaction at each hinge = $\frac{2100 \times \text{actuator force}}{(760 + 1895)}$
s	centre-to-centre spacing of transverse reinforcement (Table 1)
T	prefix for high-yield deformed bar with specified yield strength of 460 MPa (Table 1)
x	dummy variable for perpendicular distance from point of contra-flexure (Figure 7)
y	dummy variable for column curvature (Figure 7)
Δ	measured column lateral displacement
Δ_c	computed column lateral displacement from Equation 14
Δ_u	measured column lateral displacement at 0·8M_p post peak (= ultimate displacement)
Δ_y	yield displacement

Department of Civil Engineering, The University of Hong Kong (HKU), Pokfulam Road, Hong Kong.

(MACR 900102). Paper received 20 June 2009; last revised 2 September 2009; accepted 4 December 2009.

www.concrete-research.com 1751-763X (Online) 0024-9831 (Print)

Δ_1, Δ_2 column lateral displacement at $+0{\cdot}75M_u$ and $-0{\cdot}75M_u$ respectively
θ measured column rotation
θ_u ultimate column rotation
μ displacement ductility factor
ρ area ratio of longitudinal steel
ρ_s volumetric ratio of transverse steel
ϕ column curvature
$\phi(x)$ elastic curvature function
ϕ_e maximum elastic curvature
ϕ_{max} maximum column curvature
$\phi_p(x)$ inelastic curvature function
ϕ_u ultimate curvature
ϕ''_y average measured column curvature at $\pm 0{\cdot}75M_u$

Introduction

It has been verified by theoretical analyses (Bai and Au, 2009; Kim *et al.*, 2007; Kwan *et al.*, 2004; 2006; Lam *et al.*, 2009; Pam and Ho, 2001) and experimental tests (Ahn and Shin, 2007; Bayrak and Sheikh, 1998; Ho and Pam, 2003a; 2003b; Hong *et al.*, 2006; Li *et al.*, 1991; Sharma *et al.*, 2007; Watson and Park, 1994; Xiao *et al.*, 2008; Youssef and Rahman, 2007) that the flexural strength and ductility performance of reinforced concrete (RC) columns, including high-strength RC (HSRC) columns, can be improved significantly by installing a sufficient amount of transverse reinforcement to confine their concrete core. The transverse reinforcement not only averts brittle failure owing to shear, but also confines the core area to avoid premature concrete crushing and postpone inelastic buckling of longitudinal steel effectively. In the past, numerous researchers have conducted cyclic reversed loading tests on RC columns to assess their seismic performance by displacement ductility factor (Ahn and Shin, 2007; Baczkowski and Kuang, 2008; Xiao *et al.*, 2008; Youm *et al.*, 2007) or displacement as well as curvature ductility factor (Bayrak and Sheikh, 1998; Ho and Pam, 2003a; 2003b; Li *et al.*, 1991; Watson and Park, 1994) which is the ratio of the ultimate to the yield value of the respective parameter. Some theoretical analyses were also carried out to investigate the flexural ductility of RC beams and columns (Bai *et al.*, 2007; Bai and Au, 2009; Ho *et al.*, 2003; 2004; Kwan *et al.*, 2002; 2004; 2006; Kwan and Au, 2004; Lam *et al.*, 2009; Su *et al.*, 2006; 2009). In addition to ultimate curvature and ultimate displacement, ultimate rotation of the member is also important in the design of earthquake-resistant structures. Both ultimate displacement and ultimate rotation are used in this study to measure the deformability (deflection and rotation) of HSRC columns. Without knowing the deformability of a member, the redistribution of internal forces after the formation of plastic hinges during an earthquake attack cannot be predicted and the member would fail in a brittle manner (Inel *et al.*, 2007; Lam *et al.*, 2009; Spence, 2008; Wu *et al.*, 2004).

Very limited information is available on the deformability design of normal-strength RC (NSRC) and high-strength reinforced concrete (HSRC) columns because of the complicated behaviour of plastic hinges in RC structures (Bae and Bayrak, 2008; Bayrak and Sheikh, 2001; Daniell *et al.*, 2008; Haskett *et al.*, 2009; Inel and Ozmen, 2006; Jaafar, 2008; Morley, 2008). Previous experimental studies on NSRC and HSRC columns focused mainly on the flexural ductility performance (Ahn and Shin, 2007; Bayrak and Sheikh, 1998; Li *et al.*, 1991; Watson and Park, 1994). Recently, Lam *et al.* (2003) proposed an equation obtained by non-linear regression analysis based on their experimental results to predict the ultimate drift ratio of rectangular columns. However, the equation is only applicable to NSRC columns subjected to medium or high axial load level with low confinement steel content ($<0{\cdot}3\%$), which is uncommon in the design of earthquake-resistant structures. Bayrak and Sheikh (1998) proposed that the plastic hinge length of HSRC columns was about $1{\cdot}0h$, where h is the larger cross-section dimension of columns. Bae and Bayrak (2008) developed an empirical equation to predict the plastic hinge length of NSRC columns subjected to low and medium axial load levels.

Plastic hinge length is a crucial parameter in evaluating the deformability of RC columns. This length should not be confused with the 'potential plastic hinge length', which has been renamed as 'critical region length' (Ho and Pam, 2004). The former is a fictitious length in a column subjected to inelastic curvature, which is used to evaluate the column deflection for a given idealised column curvature profile, while the latter is a region in a column that needs to be confined to avert brittle failure. The critical region length in a column is generally larger than its plastic hinge length and therefore not suitable for the deformability evaluation. An investigation on the column critical region length was conducted earlier by the present authors (Ho and Pam 2004), who indicated that the extent of column region needs to be confined for providing adequate ductility.

To evaluate the deformability of HSRC columns, the following parameters are required

(*a*) plastic hinge length
(*b*) ultimate column curvature
(*c*) column curvature profile.

An idealised instead of actual column curvature profile is usually used in conjunction with the plastic hinge length since the latter is highly non-linear depending on the locations of flexural cracks as well as the onset of steel buckling and/or yielding.

In the current paper, the plastic hinge lengths of eight HSRC columns are evaluated using an idealised column curvature profile proposed by Park and Paulay

(1975). In this profile, the measured ultimate curvature of each column specimen is adopted to give a closer agreement between the calculated column rotation and deflection (obtained from the idealised curvature profile) and their respective measured values. For the purpose of design, two formulae are proposed. The first formula relates the plastic hinge length to the column cross-section dimension, content of longitudinal and transverse steel, axial load level, concrete strength and transverse steel yield strength, whereas the second formula relates the ultimate curvature of the column to the same parameters. With the plastic hinge length and ultimate column curvature, the rotation and deflection capacities of the column can be obtained from the integration of, respectively, the area and first moment of area of the idealised curvature profile. To verify the validity of the proposed formulae, deflections of other researchers' column specimens are evaluated and compared with their respective measured values.

Experimental programme

In the present study, eight column specimens were fabricated and tested. The details, instrumentation and test procedure relating to the column specimens are explained next.

Details of test specimens

The perspective view and loading arrangement of a typical test specimen are shown in Figure 1, and Table 1 summarises the properties of the column specimens. Each of the column specimens has a square cross-section of 325 mm and a clear height of 1515 mm; the latter represents the real column situation in a RC moment-resisting framed building between contra-flexure point (around storey mid-height) and maximum bending moment point (at the beam–column joint).

The transverse steel in terms of volumetric ratio ρ_s in each column specimen within its critical region length (L_{CR}) was designed using the present authors' proposed equation for limited ductile HSRC columns (Ho and Pam, 2003a; 2003b). In evaluating ρ_s, the specified values of material strengths were used. The transverse steel outside the critical region was designed to be just sufficient to resist the ultimate shear force. The extent of the critical region (L_{CR}) in the column specimens followed that proposed by the authors for HSRC columns (Ho and Pam, 2004), that is

(*a*) 2·0 times the cross-section dimension ($\approx$ 650 mm) for specimens subjected to a large compressive axial load level ($P/A_g f'_c$ about 0·6); units 1, 5 and 8 belong to this category
(*b*) 1·5 times the cross-section dimension ($\approx$ 500 mm) for specimens subjected to a medium compressive axial load level ($P/A_g f'_c$ between 0·3 and 0·6); units 2, 4, 6 and 7 belong to this category
(*c*) 1·0 times the cross-section dimension (= 325 mm) for the specimen subjected to a low compressive axial load level ($P/A_g f'_c$ between 0·1 and 0·3); unit 3 belongs to this category.

To facilitate the application of reversed cyclic bending moment induced by a pair of actuator forces, a horizontal rigid beam was fabricated monolithically at one end of each column specimen (Figure 1). As the maximum moment was meant to occur at the beam–column interface, each of the horizontal rigid beams was designed to be much stronger than the column, so that it behaved elastically throughout the test.

At the other end of the column, a flange was designed and fabricated monolithically to facilitate connection to the top hinge of the loading frame (Figure 1), where it formed the point of contra-flexure.

Instrumentation

Seven pairs of linear variable displacement transducers (LVDTs) were installed on each of the two extreme faces of every column to measure curvature profiles, as illustrated in Figure 2. The pair located at 25 mm above the beam–column interface functioned to measure the maximum column curvature. In addition, one LVDT was installed at the column flange to measure the column lateral displacement, one pair of LVDTs was installed at each of the top and bottom hinges to measure the column rotation. Readings from these additional LVDTs were used in the back analysis to evaluate the column plastic hinge length. Figure 2 illustrates the LVDT arrangement.

There were other types of instrumentation used in the test but these are not discussed in the present paper because they had no direct impact on the parameters evaluated in this study. The complete details of the rest of the instrumentation are described elsewhere (Ho, 2003).

Test procedure

Each of the column specimens was subjected to an axial compression load, which was held more or less constant throughout the test, and reversed cyclic bending moment simultaneously. In the first cycle, the column was maintained elastic and loaded to $+0{\cdot}75M_u$ and $-0{\cdot}75M_u$ (clockwise and anticlockwise directions respectively), where M_u is the column flexural strength calculated based on Eurocode 2 (CEN, 2004) using the actual values of f'_c, f_y and P. The respective column lateral displacements were recorded as Δ_1 and Δ_2, from which the yield displacement Δ_y is obtained, that is

$$\Delta_y = \frac{4}{3}\left(\frac{\Delta_1 + |\Delta_2|}{2}\right) \quad (1)$$

The subsequent cycles were displacement-controlled. In the second cycle, the column lateral displacement Δ was increased to Δ_y and then $-\Delta_y$, which were equiva-

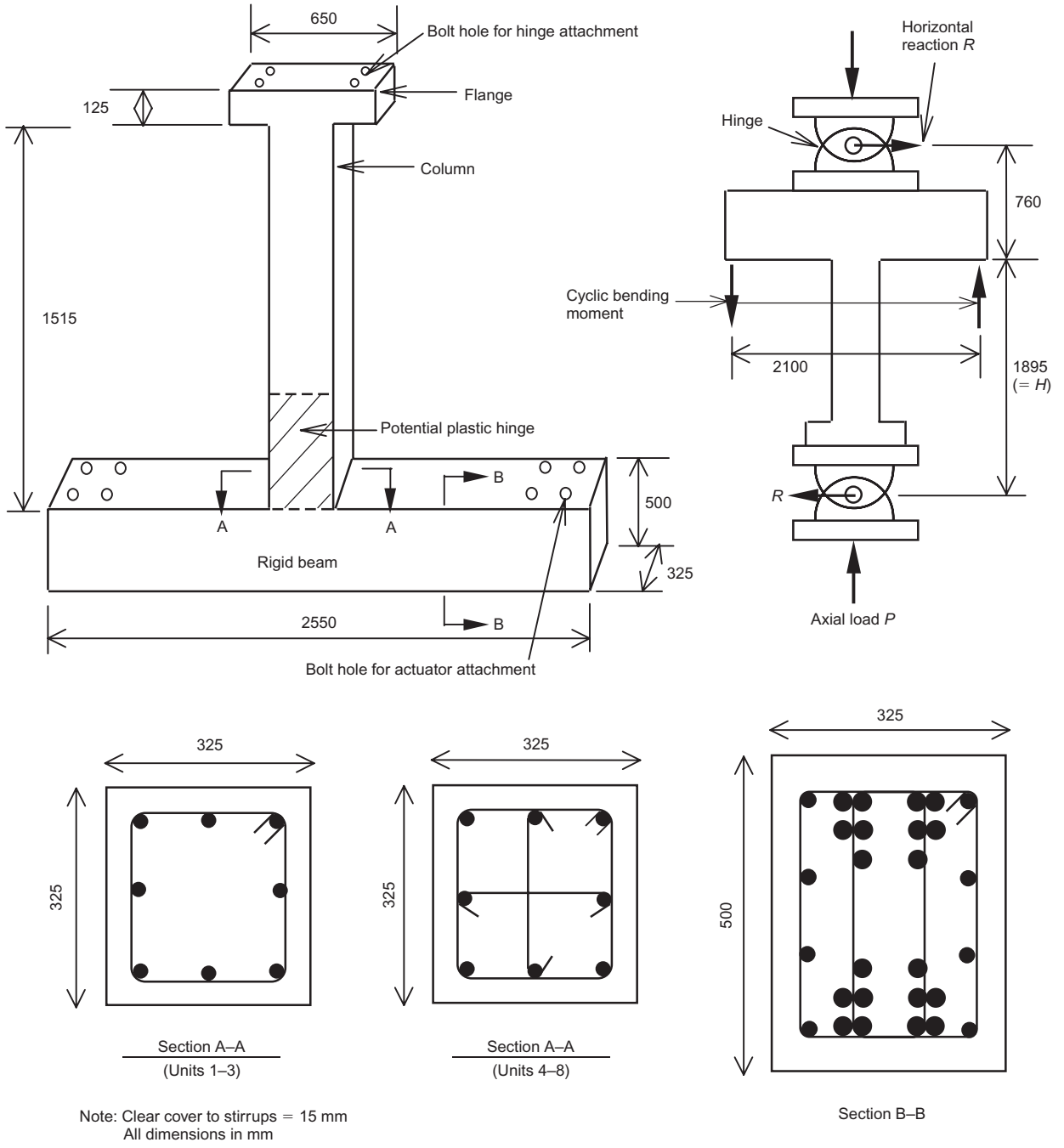

Figure 1. Detail of test specimens and loading arrangement

lent to $\mu = +1$ and -1, respectively, where μ is the displacement ductility factor given by

$$\mu = \Delta/\Delta_y \tag{2}$$

Afterwards, Δ was increased by Δ_y every two cycles, in which the repeated cycle was to observe the flexural strength degradation in the column. The process was repeated until the measured moment capacity in the column dropped to less than 80% of the measured maximum moment M_p.

Test results and discussion

In this section, the envelopes of moment–lateral displacement, moment–curvature and moment–rotation will be discussed. Each of the envelopes was obtained from the corresponding hysteresis curves. The ultimate values of column lateral displacement, curvature and rotation will be defined accordingly. These ultimate values will be adopted at a later stage to calculate the column rotation and deflection.

Measured moment–lateral displacement envelopes

Figure 3 shows the moment–lateral displacement envelopes for all of the column specimens. The mo-

Table 1. Properties of column specimens

Unit code*	Actual f'_c: MPa	Average $P/A_g f'_c$	L_{CR}: mm	f_{ys}: MPa	Longitudinal steel		Transverse steel		
					Content	ρ: %	d_s: mm	s:† mm	ρ_s:‡ %
60-06-61-S	50·0	0·61	650	531	8T32	6·1	T12	70	2·10 (0·38)
100-03-24-S	83·3	0·33	500	531	8T20	2·4	T12	70	2·10 (0·66)
80-01-09-S	77·8	0·12	325	339	8T12	0·9	R12	85	1·73 (0·38)
80-03-24-C	80·6	0·31	500	531	8T20	2·4	T12	105	2·10 (0·38)
60-06-61-C	56·1	0·59	650	531	8T32	6·1	T12	110	2·00 (0·47)
100-03-24-C	96·4	0·34	500	531	8T20	2·4	T12	90	2·45 (0·66)
100-03-61-C	94·7	0·35	500	531	8T32	6·1	T12	100	2·20 (0·66)
100-06-61-C	85·0	0·63	650	572	8T32	6·1	T16	120	3·20 (0·66)

* Code explanation: in the code number 100-03-24-C, for example, 100 represents specified concrete cube strength (= 100 MPa); 03 represents specified compressive axial load level, $P/A_g f'_c$ (= 0·3); 24 represents longitudinal steel ratio, ρ (= 2·4%); and the letter C indicates cross ties added, whereas S would signify single closed hoops.
† For ease of construction, minimum s is set at 70 mm.
‡ ρ_s values in parenthesis are for outside critical region.

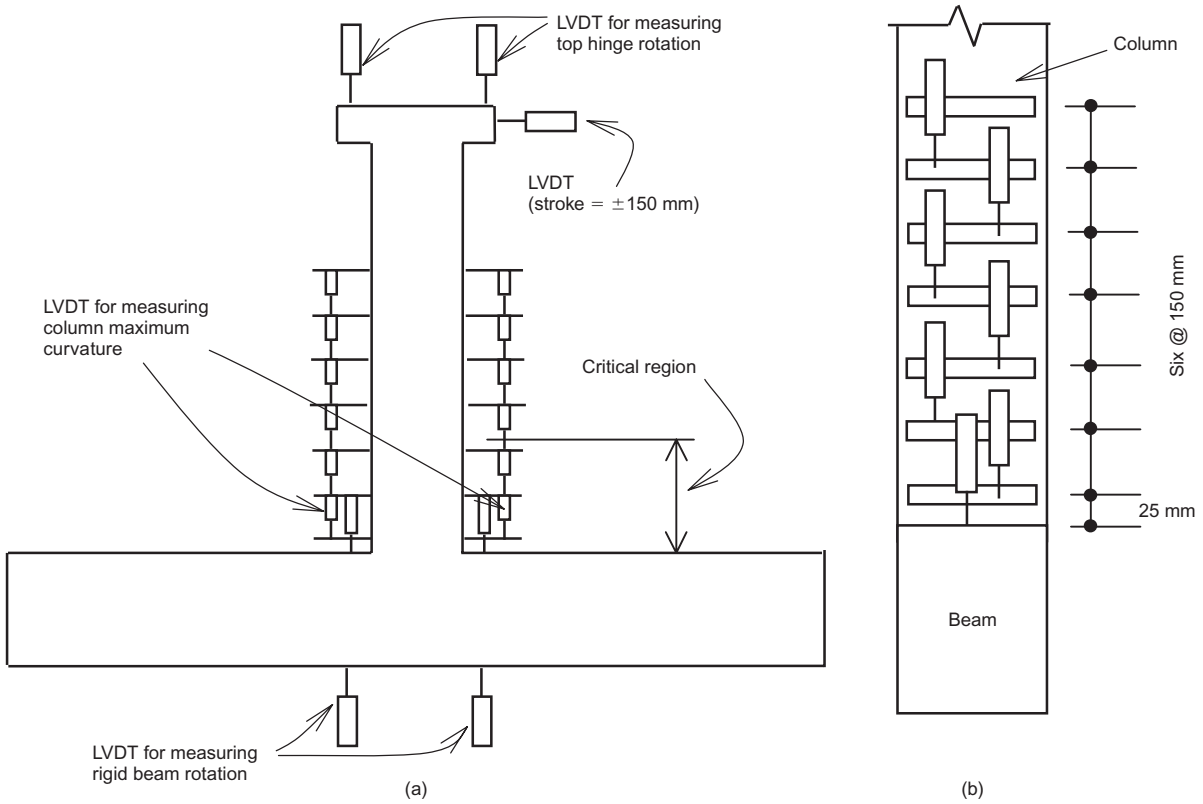

Figure 2. LVDT arrangement: (a) front elevation; (b) side elevation

ment was obtained at the beam–column interface, that is 1·895R kN m, where R is the horizontal reaction at the hinge and 1·895 m is the distance from the bottom hinge to the beam–column interface (see Figure 1). In Figure 3, the value of theoretical moment M_u (without taking into account the P–Δ effect) is shown as a solid horizontal line and that with the P–Δ effect is shown as an inclined dotted line.

Although after failure some of the column specimens could still experience many more inelastic cycles with reasonable energy dissipation capability, their load-carrying capacity could not be maintained above $0{\cdot}8M_p$. Failure was considered to have been reached when the load-carrying capacity dropped to 80% of M_p, and the corresponding column lateral displacement at this stage is defined as ultimate column lateral displacement Δ_u. It should be noted that since the measured flexural strength M_p was always higher than the theoretical strength M_u due to the confinement effect (Pam and Ho, 2001), M_p was used in the failure criterion in order not to overestimate the ductility factor. The values of Δ_u are listed in Table 2. These values will be

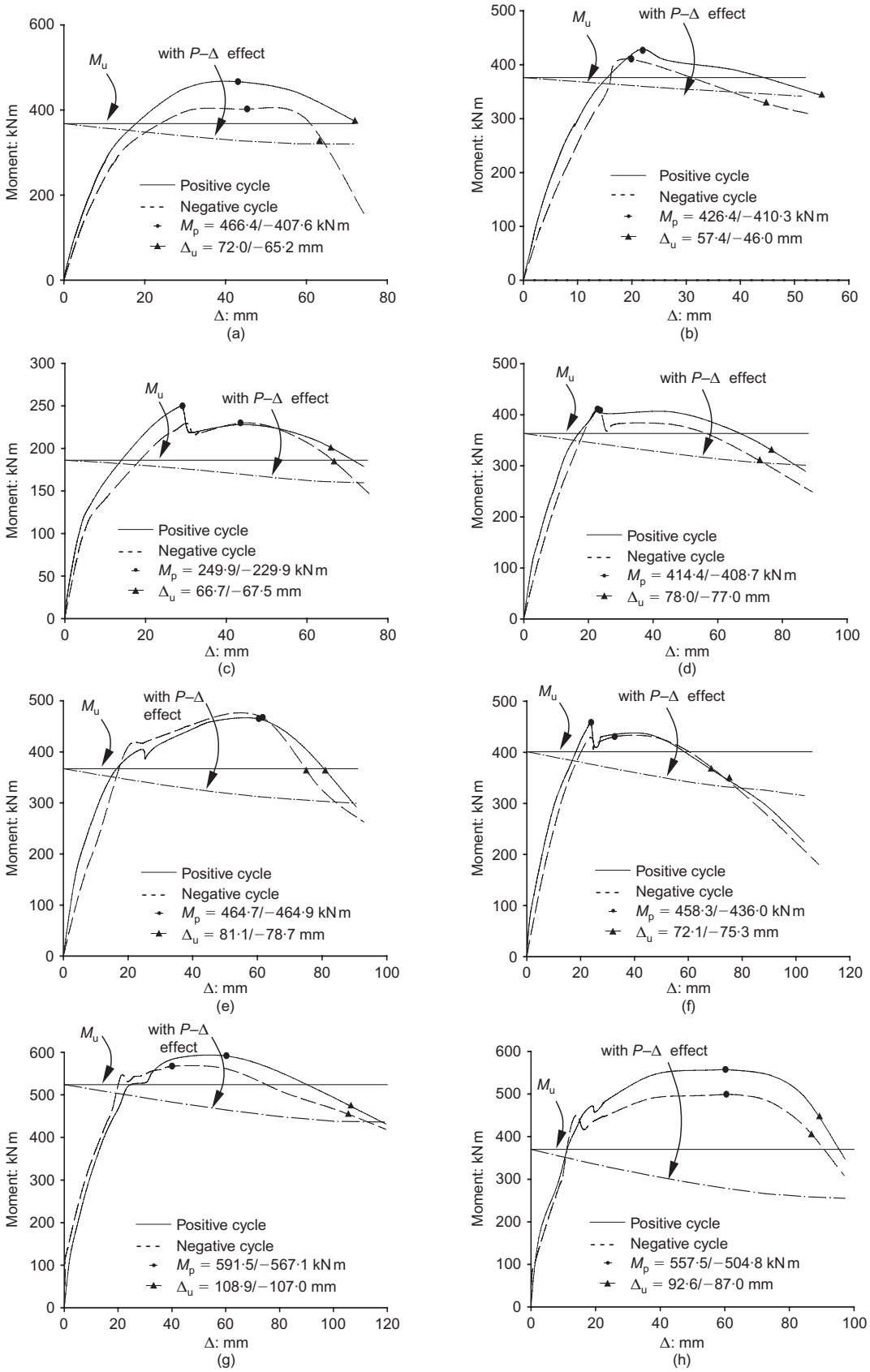

Figure 3. Measured moment–lateral displacement envelopes: (a) unit 1: 60-06-61-S; (b) unit 2: 100-03-24-S; (c) unit 3: 80-01-09-S; (d) unit 4: 80-03-24-C; (e) unit 5: 60-06-61-C; (f) unit 6: 100-03-24-C; (g) unit 7: 100-03-61-C; (h) unit 8: 100-06-61-C

Table 2. Plastic hinge lengths of column specimens

Unit code	Average $P/A_g f'_c$	ρ_s: %	ϕ_e: rad/m	ϕ_u: rad/m	θ_u: rad	Δ_u: mm	ℓ_p: mm, obtained from		
							Equation 8	Equation 11	Equation 12b
60-06-61-S	0·61	2·10	0·0126	0·1230	0·0558	68·6	399	373	255
100-03-24-S	0·33	2·10	0·0100	0·1205	0·0396	51·7	274	268	253
80-01-09-S	0·12	1·73	0·0081	0·2233	0·0523	67·1	208	187	196
80-03-24-C	0·31	2·10	0·0113	0·1481	0·0591	77·5	355	351	238
60-06-61-C	0·59	2·00	0·0102	0·1552	0·0595	79·9	345	348	296
100-03-24-C	0·34	2·45	0·0105	0·1121	0·0586	73·7	481	471	288
100-03-61-C	0·35	2·20	0·0122	0·1726	0·0910	108·2	497	448	447
100-06-61-C	0·63	3·20	0·0112	0·1635	0·0710	89·8	398	377	385

used to evaluate the column plastic hinge lengths using back calculation.

Measured moment–curvature envelopes

The column curvature ϕ was calculated based on the difference of the strain values between the pair of LVDTs located at 25 mm above the beam–column interface, divided by their horizontal distance. Each of the strain values was obtained from the corresponding LVDT reading divided by its gauge length. The column curvatures are plotted against the measured moments to form hysteresis curves, and the resulting envelope for each specimen in the positive cycle is shown in Figure 4.

The ultimate curvature ϕ_u is defined as the curvature at which the moment capacity has declined to 80% of M_p in the post-peak branch. Figure 5 illustrates schematically how to obtain the ultimate curvature. The values of ϕ_u are listed in Table 2 and they will be used in the evaluation of the column plastic hinge lengths using the two proposed indirect methods, which are explained later.

Measured moment–rotation envelopes

Figure 6 shows envelopes of the measured moment against the column rotation (θ) hysteresis curves in the positive cycle. The column rotation is the difference of rotation between the hinges connected to the rigid beam and to the column end, respectively(see Figure 7). The ultimate column rotation θ_u is shown in Figure 6; this will be used to determine the column plastic hinge lengths in one of the proposed indirect methods using back calculation. The ultimate column rotation θ_u for each specimen was obtained in a similar manner to the ultimate curvature explained in Figure 5; this is also listed in Table 2.

Plastic hinge length evaluation based on indirect methods

It is proposed to evaluate the column plastic hinge length by back calculation based on its measured rotation using the column curvature profile. This method is referred to in this paper as 'the first indirect method'. Using the similar procedure, 'the second indirect method' utilises the measured column lateral deflection. Instead of using the measured column curvature distribution obtained from the experiment, which consists of only discrete points rather than a continuous distribution, it is decided to adopt the idealised curvature profile proposed by Park and Paulay (1975). The advantage of using the idealised curvature profile is simplicity, because it is defined by only three parameters, that is plastic hinge length ℓ_p, maximum elastic curvature ϕ_e and maximum column curvature ϕ_{max} (see Equations 4 and 5 and Figure 7). Furthermore, the idealised curvature profile has been proven to predict fairly accurately the plastic hinge rotation in NSRC columns (Watson and Park, 1994).

Idealised column curvature profile

Figure 7 shows the idealised curvature profile along the column height comprising two portions, namely elastic and inelastic curvature distributions. The elastic curvature distribution is represented by a straight line joining the point of contra-flexure, where the curvature is zero, and the point of maximum moment, where the curvature is ϕ_e. The value of ϕ_e, as proposed by Park and Paulay (1975), is defined as the column curvature at M_u, obtained from extrapolating the average measured column curvature at $\pm 0{\cdot}75M_u$, that is ϕ''_y, as follows

$$\phi_e = \phi''_y / 0{\cdot}75 \tag{3}$$

The ϕ_e value for each of the column specimens is listed in Table 2.

The inelastic curvature profile covers only the plastic hinge region, with its slope similar to that of the elastic curvature profile, and ϕ_{max} is the maximum column curvature at the beam–column interface, which is equal to ϕ_u at the ultimate state.

Both the elastic and inelastic curvature distributions could be represented mathematically by, respectively, elastic curvature function, $\phi(x)$, and inelastic curvature function, $\phi_p(x)$, where x is a distance along the column height from the point of contra-flexure. Both the functions and their valid ranges are expressed as follows

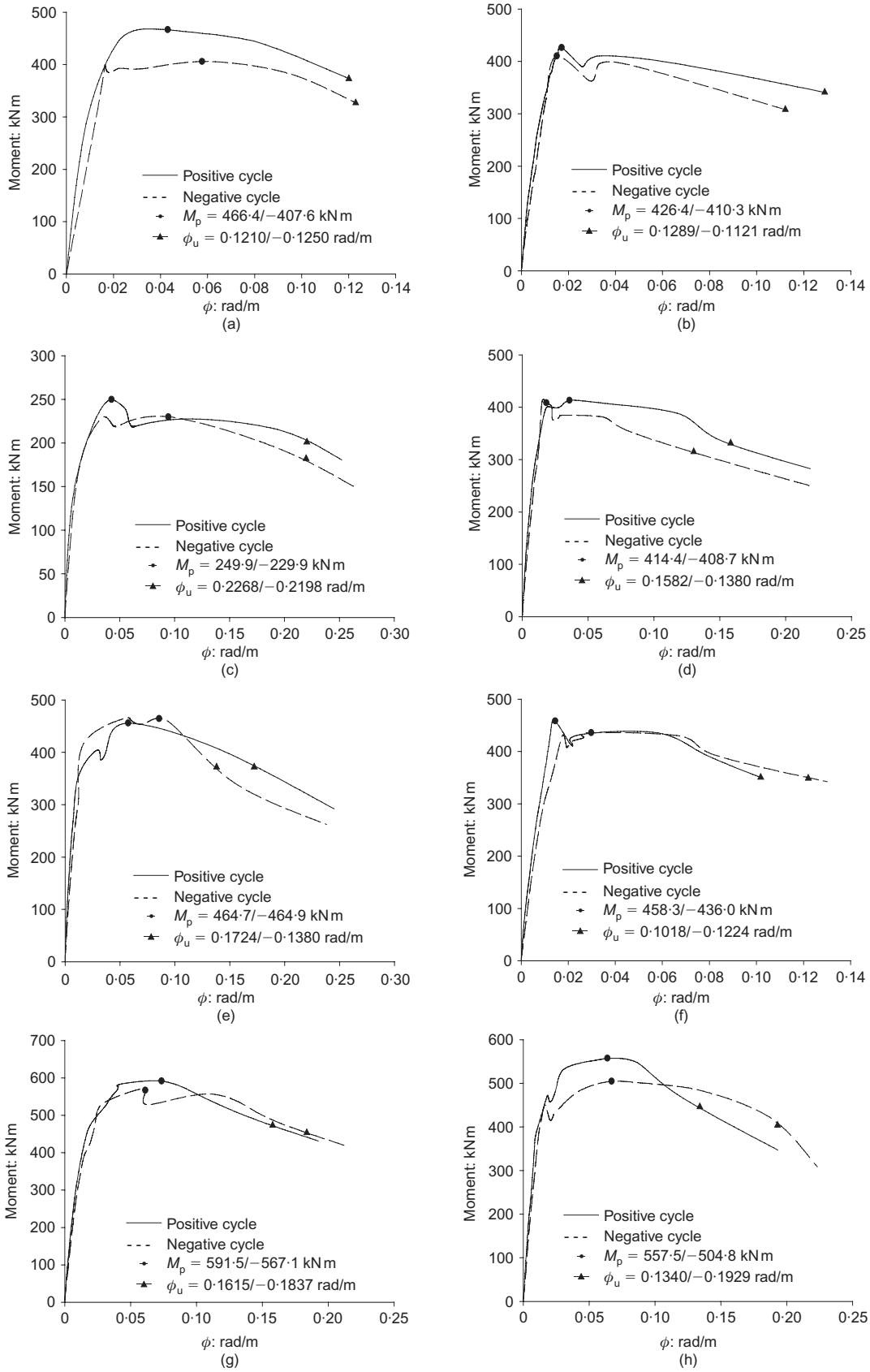

Figure 4. Measured moment–curvature envelopes: (a) unit 1: 60-06-61-S; (b) unit 2: 100-03-24-S; (c) unit 3: 80-01-09-S; (d) unit 4: 80-03-24-C; (e) unit 5: 60-06-61-C; (f) unit 6: 100-03-24-C; (g) unit 7: 100-03-61-C; (h) unit 8: 100-06-61-C

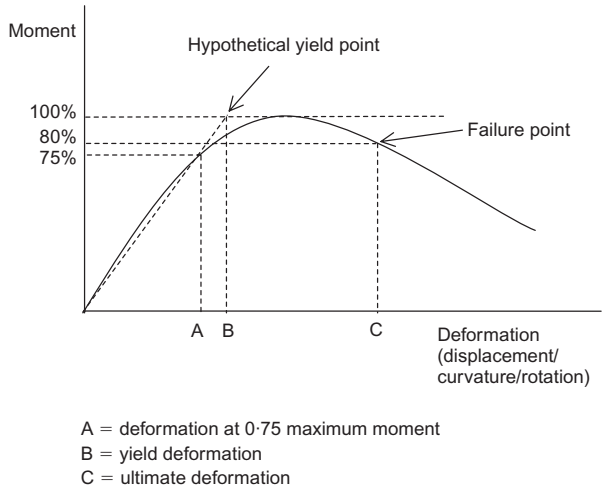

Figure 5. Definition of ultimate and yield deformations

$$\varphi(x) = \frac{\varphi_e}{H}x \qquad \forall \quad 0 \leqslant x \leqslant H \quad (4)$$

$$\varphi_p(x) = \begin{cases} 0 & \forall\ 0 \leqslant x < H - \ell_p \\ \dfrac{\varphi_e}{H}x + (\varphi_{max} - \varphi_e) & \forall H - \ell_p \leqslant x \leqslant H \end{cases} \quad (5)$$

where H (= 1895 mm in this study) is the distance from the point of contra-flexure to the beam–column interface or the point of maximum bending moment. Although there should be a sudden change in the column curvature at the interface of the column and the flange at the column end, it is neglected in the present study because the elastic curvature at that section is negligible.

Back analysis based on measured column rotation (indirect method 1)

From the idealised column curvature profile (Figure 7), ℓ_p of the column specimens could be evaluated from first principles using back calculation. However, since ℓ_p increases gradually with the column lateral deformation in the post-peak stage, it is decided in this study to evaluate only ℓ_p at the ultimate state ($0{\cdot}8M_p$ post peak).

In the first indirect method, ℓ_p at the ultimate state is evaluated using the measured column rotation and the idealised curvature profile. From the moment area method, the total column rotation at any loading stage is equal to the total area under the corresponding column curvature profile, which is expressed as

$$\theta = \int_{H''}^{H} \varphi(x)\mathrm{d}x + \int_{H-\ell_p}^{H} [\varphi_p(x) - \varphi(x)]\mathrm{d}x \quad (6)$$

where the first and second terms represent respectively the elastic and inelastic rotations in the column and H'' is the distance from the point of contra-flexure to the top of the column flange (Figure 7). Substituting Equations 4 and 5 into Equation 6, and assuming the column has reached the ultimate state, Equation 6 becomes

$$\theta_u = \frac{1}{2H}\varphi_e(H^2 - H''^2) + (\varphi_u - \varphi_e)\ell_p \quad (7)$$

After rearranging, the column plastic hinge length could be expressed as

$$\ell_p = \frac{\theta_u - (1/2H)\varphi_e(H^2 - H''^2)}{\varphi_u - \varphi_e} \quad (8)$$

For each column specimen, the values of ϕ_u and θ_u are obtained from its respective measured moment–curvature and measured moment–rotation envelopes as shown in Figures 4 and 6. The values of ϕ_e are obtained from Equation 3. The resulting column plastic hinge lengths are listed in Table 2, together with all the contributing parameters.

Back analysis based on measured lateral displacement (indirect method 2)

In the second indirect method, ℓ_p at the ultimate state is evaluated using the measured column lateral displacement and the idealised curvature profile. From the moment area method, if the interface of the column and the rigid beam is assumed to be a fixed support and the point of contra-flexure is assumed to be a free end, then the lateral deflection with respect to the fixed support measured at an arbitrary point on the column is equal to the first moment of area of the idealised curvature profile about that point, extending from the point of contra-flexure to the point where the lateral deflection is measured. The measured column lateral displacement at any point having a distance x from the point of contra-flexure is expressed as

$$\Delta = \int_{H'}^{H} (x - H')\varphi(x)\mathrm{d}x + \int_{H-\ell_p}^{H} (x - H')[\varphi_p(x) - \varphi(x)]\mathrm{d}x \quad (9)$$

where H' is the distance from the point of contra-flexure to the point where the maximum lateral displacement is measured (Figure 7). In Equation 9, the first and second terms denote respectively the elastic and inelastic contribution towards the deflection. By substituting Equations 4 and 5 into Equation 9, the integration will yield Δ_u as follows

$$\Delta_u = \left(\frac{1}{3}H^3 - \frac{1}{2}H'H^2 + \frac{1}{6}H'^3\right)\frac{\varphi_e}{H} + (\varphi_u - \varphi_e)\left(H - H' - \frac{\ell_p}{2}\right)\ell_p \quad (10)$$

The above is a quadratic equation in ℓ_p, which can be solved by the well-known quadratic formula as follows

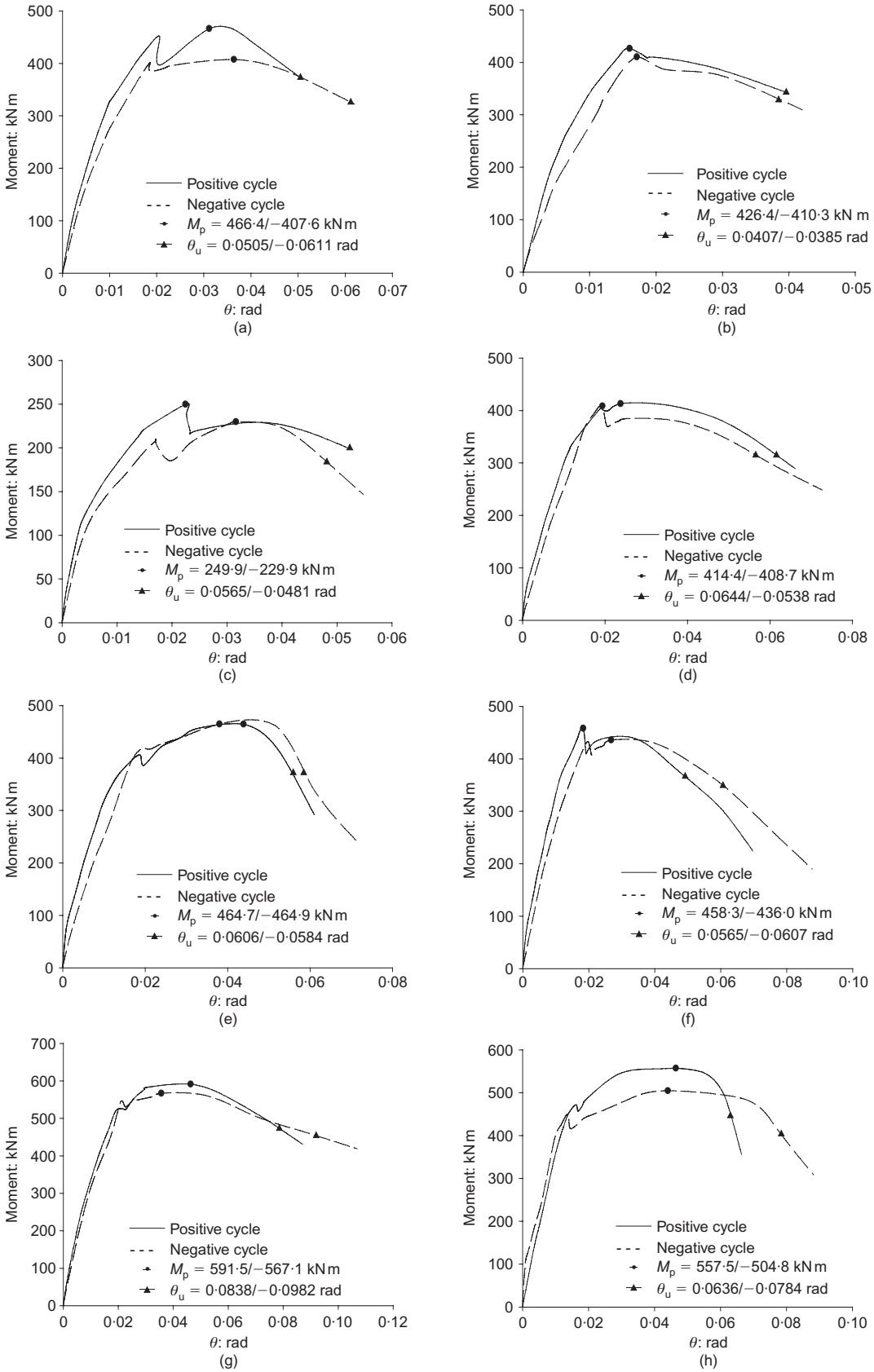

Figure 6. Measured moment–rotation envelopes: (a) unit 1: 60-06-61-S; (b) unit 2: 100-03-24-S; (c) unit 3: 80-01-09-S; (d) unit 4: 80-03-24-C; (e) unit 5: 60-06-61-C; (f) unit 6: 100-03-24-C; (g) unit 7: 100-03-61-C; (h) unit 8: 100-06-61-C

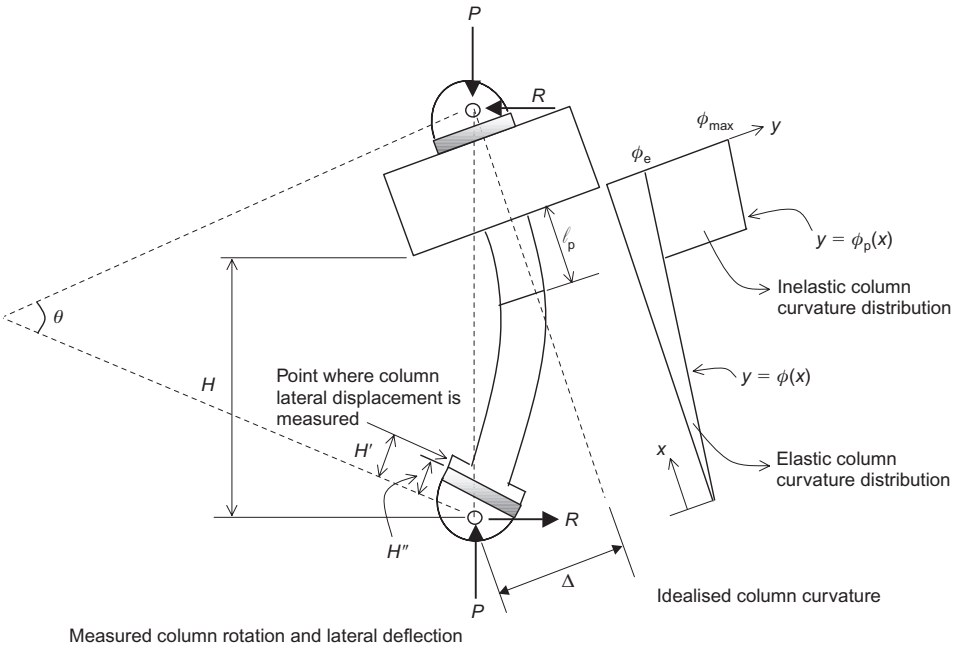

Figure 7. Column deflected shape and idealised curvature profile

$$\ell_p = \frac{-B \pm \sqrt{(B^2 - 4AC)}}{2A} \tag{11}$$

where

$$A = \frac{\varphi_u - \varphi_e}{2}$$

$$B = -(\varphi_u - \varphi_e)(H - H')$$

and

$$C = \Delta_u - \left(\frac{1}{3}H^3 - \frac{1}{2}H'H^2 + \frac{1}{6}H'^3\right)\frac{\varphi_e}{H}$$

The smaller positive root given by Equation 11 is adopted as the plastic hinge length, whose value for each of the column specimens is listed in Table 2.

From Table 2, it is obvious that the plastic hinge lengths evaluated using both the indirect methods are in close agreement, with those obtained from the rotation (indirect method 1) being slightly larger than those obtained from the displacement (indirect method 2).

Proposed evaluation method for column deformability

The evaluation of column rotation and deflection is based on integration of the area and first moment of area, respectively, of its idealised curvature profile. Three parameters are required to shape the curvature profile: plastic hinge length (ℓ_p), maximum elastic curvature (ϕ_e) and ultimate curvature (ϕ_u). Among these parameters, plastic hinge length and ultimate curvature are relatively more important in the deformability prediction. Therefore, two equations are proposed to relate these two parameters to the other contributing parameters.

Proposed plastic hinge length for design

The plastic hinge lengths obtained for HSRC columns presented in this study have been correlated to various structural parameters using regression analysis. From previous investigations (Bae and Bayrak, 2008; Bayrak and Sheikh, 2001; Inel and Ozmen, 2006), the major factors affecting the plastic hinge length of HSRC columns are

(*a*) compressive axial load level
(*b*) longitudinal and transverse steel volumetric ratios
(*c*) concrete strength.

Thus, by incorporating all these factors, the column plastic hinge length (in dimensionless form) could be expressed as

$$\frac{\ell_p}{h} = k_1\left(\frac{P}{A_g f'_c}\right)^{\alpha}\left(\frac{f'_c}{f_{ys}}\right)^{\beta}\left(\frac{\rho}{\rho_s}\right)^{\gamma} + k_2 \tag{12a}$$

where k_1, k_2, α, β and γ are real constants to be determined by regression analysis and h is the larger cross-section dimension of the column. It was decided to use the average plastic hinge length obtained from both the indirect methods of each column specimen for the regression analysis. The values of α, β and γ were determined by regression analysis. In determining each of these values, the index to be determined is varied while other parameters are kept constant, such that the best correlation coefficient is obtained. Having determined the values of $\alpha = 0{\cdot}5$, $\beta = 1{\cdot}5$ and $\gamma = 0{\cdot}5$ that gave the best correlation, the values of k_1 and k_2 were

obtained from the regression analysis. For conservative prediction of the deformability of HSRC columns, it is proposed to fit a lower bound equation for the obtained plastic hinge lengths. This lower bound equation is plotted in Figure 8 and expressed as follows

$$\frac{\ell_p}{h} = 16{\cdot}5\left(\frac{P}{A_g f'_c}\right)^{0{\cdot}5}\left(\frac{f'_c}{f_{ys}}\right)^{1{\cdot}5}\left(\frac{\rho}{\rho_s}\right)^{0{\cdot}5} + 0{\cdot}15 \quad (12b)$$

where the constants 16·5 and 0·15 are respectively k_1 and k_2.

The results from Equation 12b based on the actual material properties of all the column specimens are listed in Table 2 and compared with the plastic hinge lengths obtained from both the indirect methods. As expected, the predicted plastic hinge lengths obtained from Equation 12b are mostly smaller than those obtained from both the indirect methods and so will be the resulting deformability (rotations or deflections).

Proposed maximum elastic curvature for design

From Table 2, it is evident that the values of maximum elastic curvature ϕ_e for various columns vary within a narrow range from 0·0081 to 0·0126 rad/m. For practical design purposes in evaluating column deformability, it is proposed to use a fixed value of $\phi_e = 0{\cdot}01$ rad/m, which is the average value of obtained ϕ_e.

Proposed equation of ultimate curvature for design

Another parameter that must be known before evaluating the column deformability is ultimate curvature ϕ_u. Therefore, it is proposed to relate ϕ_u to the contributing parameters by the following equation

$$\varphi_u h = k_1\left(\frac{P}{A_g f'_c}\right)^{\alpha}\left(\frac{f'_c}{f_{ys}}\right)^{\beta}\left(\frac{\rho}{\rho_s}\right)^{\gamma} + k_2 \quad (13a)$$

By using the same derivation approach as adopted in Equation 12b, the values of α, β and γ were determined as 1·0, 2·0 and 1·0 respectively. Subsequently, the values of k_1 and k_2 were obtained from the regression analysis, as shown in Figure 9.

In a similar approach to that used for plastic hinge length, for conservative prediction of the deformability of HSRC columns, it is proposed to fit a lower bound equation for the obtained ultimate curvatures. This lower bound equation is plotted in Figure 9 and expressed as follows

$$\varphi_u h = 0{\cdot}86\left(\frac{P}{A_g f'_c}\right)\left(\frac{f'_c}{f_{ys}}\right)^2\left(\frac{\rho}{\rho_s}\right) + 0{\cdot}026 \quad (13b)$$

Verification against other researchers' results

Equations 12b and 13b are verified against the test results obtained by other researchers with the help of the idealised curvature profile. Measured lateral deflections of columns from Bae and Bayrak (2008), Bayrak and Sheikh (1998), Marefat *et al.* (2006), Paultre *et al.* (2001), Sheikh and Yeh (1990), Sheikh *et al.* (1994) and Woods *et al.* (2007) and were selected for comparison with their corresponding theoretical deflections computed using Equations 12b and 13b.

In calculating the above theoretical lateral deflections, the actual material strengths of the column specimens were adopted. The column specimens were all of square cross-section. It is noted in the test set-up of these specimens that the dimension H' is considerably less than H, and therefore Equation 10 in this case can be simplified to

$$\Delta_c = \frac{1}{3}\varphi_e H^2 + (\varphi_u - \varphi_e)\left(H - \frac{\ell_p}{2}\right)\ell_p \quad (14)$$

The column deflections computed from Equation 14, denoted as Δ_c, are listed in Table 3, in which ℓ_p is evaluated from Equation 12b, ϕ_u is evaluated from Equation 13b and ϕ_e is equal to 0·01 rad/m. Listed also in the same table are the values of Δ_u obtained by the researchers at $0{\cdot}8M_p$ in the post-peak range of the moment–lateral displacement curve.

From Table 3, it is evident that the predicted lateral deflections of the columns are close to and mostly smaller than the actual deflection of columns measured

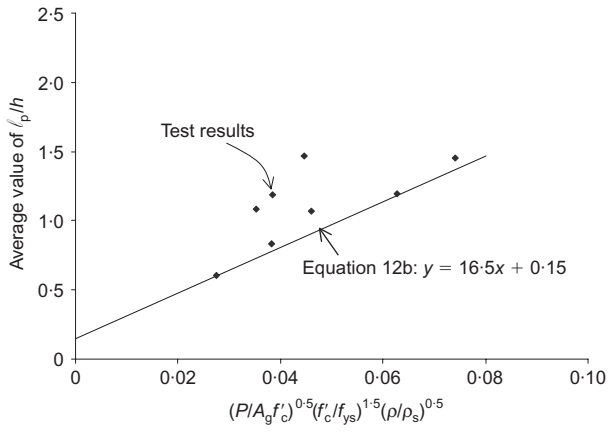

Figure 8. Proposed equation for plastic hinge length

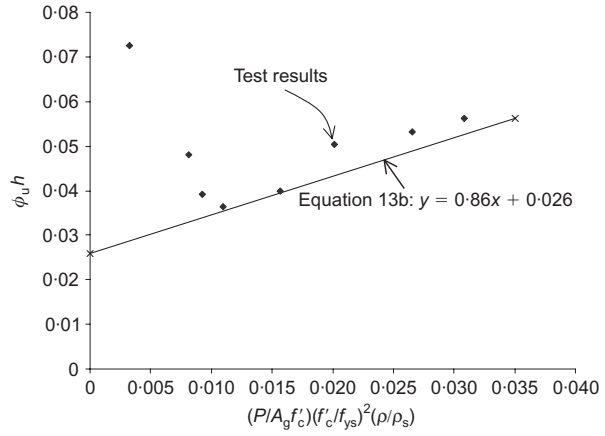

Figure 9. Proposed equation for ultimate curvature

Table 3. Comparison of the predicted and measured column deflections of other researchers

Unit code	f'_c: MPa	Average $P/A_g f'_c$	f_{ys}: MPa	ρ_s: %	ρ: %	Measured deflection Δ_u: mm	Predicted deflection Δ_c: mm	$\frac{\Delta_u}{\Delta_c}$
Bae and Bayrak (2008)								
S24-2UT	43·4	0·50	427	2·04	1·25	79·3	67·3	1·18
S17-3UT	43·4	0·50	496	1·76	1·25	61·0	63·5	0·96
S24-4UT	36·5	0·20	455	0·72	1·25	91·5	60·4	1·51
S24-5UT	41·4	0·20	434	1·30	1·25	91·5	59·3	1·54
Woods *et al.* (2007)								
S6·4-76	69·0	0·16	414	0·16	2·58	25·5	24·5	1·04
S8·0-76	69·0	0·16	414	0·16	2·58	24·4	19·6	1·24
V5·5-66	69·0	0·16	414	0·16	2·58	29·2	25·8	1·13
V6·4-86	69·0	0·16	414	0·16	2·58	28·3	25·7	1·10
Marefat *et al.* (2006)								
NBCC12	25·2	0·23	220	0·66	2·50	45·0	48·9	0·92
NBCM11	24·5	0·24	220	0·88	2·26	48·8	40·1	1·22
STCM9	24·0	0·19	220	1·20	2·00	31·5	30·5	1·03
SBCM8	28·0	0·22	220	1·10	3·00	45·8	46·3	0·99
SBCC7	27·0	0·16	220	1·10	3·00	52·5	38·2	1·37
Paultre *et al.* (2001)								
C80B60N40	78·7	0·40	438	4·26	2·15	61·7	59·6	1·04
C100B60N40	98·2	0·39	418	4·26	2·15	76·8	82·8	0·93
Bayrak and Sheikh (1998)								
AS-2HT	71·7	0·36	542	2·84	2·58	40·0	32·0	1·25
AS-4HT	71·9	0·50	463	5·12	2·58	35·3	34·2	1·03
AS-6HT	101·9	0·46	463	6·74	2·58	43·2	44·5	0·97
Sheikh *et al.* (1994)								
AS-3H	54·1	0·62	507	1·68	2·44	45·7	39·3	1·16
AS-18H	54·7	0·64	464	3·06	2·44	41·9	33·9	1·24
AS-20H	53·6	0·64	464	4·30	2·44	55·9	28·9	1·93
Sheikh and Yeh (1990)								
F-6	27·2	0·75	483	1·68	2·44	19·1	19·5	0·98
D-7	26·2	0·78	469	1·62	2·58	21·6	20·1	1·08
F-9	26·5	0·77	490	1·68	2·44	25·4	19·0	1·34
E-10	26·3	0·77	490	1·68	2·44	20·3	18·9	1·07
A-11	27·9	0·74	469	0·77	2·44	25·4	26·8	0·95
E-13	27·2	0·74	483	1·69	2·44	20·3	19·4	1·05
D-14	26·9	0·75	462	0·81	2·58	30·5	26·3	1·16
D-15	26·2	0·75	490	1·68	2·58	17·8	19·0	0·94
A-16	33·9	0·61	558	0·77	2·44	22·9	25·0	0·91
Average								1·14

in the experiment. The average underestimation obtained in Table 3 is about 14%, which is considered appropriate for deformability design of HSRC columns. The accuracy of the proposed equations for deformability evaluation of columns subjected to different axial load levels is also investigated. For columns subjected to low axial load level (i.e. $0 < P/A_g f'_c \leqslant 0{\cdot}2$), the predicted deformability of columns was underestimated by 25%. For columns subjected to medium axial load level (i.e. $0{\cdot}2 < P/A_g f'_c \leqslant 0{\cdot}6$), the predicted deformability of columns was underestimated by 5%. For columns subjected to high axial load level (i.e. $P/A_g f'_c > 0{\cdot}6$), the predicted deformability of columns was underestimated by 15%. These levels of underestimation are considered acceptable for practical deformability design of HSRC columns.

Conclusions

The plastic hinge length of eight HSRC columns for predicting column deformability was investigated experimentally. Two indirect methods based on back calculation of column rotation and deflection, respectively, were proposed for assessing the column plastic hinge length. It is evident that a good agreement was achieved between the evaluated plastic hinge lengths from both the indirect methods.

To predict column deformability at an early design stage based on a prescribed idealised curvature profile, a value of maximum elastic curvature and empirical equations for plastic hinge length and ultimate column curvature were proposed based on the test results of eight HSRC columns. From verification on the HSRC columns of other researchers, it is clear that their theoretical column deflections evaluated using the proposed method are mostly slightly smaller than their respective measured deflections. This gives a conservative prediction of column deflection in terms of ductility capacity. For HSRC columns of a square-shaped cross-section, the proposed formulae can therefore be used for rapid evaluation of HSRC column deformability at an early design stage without needing to perform the tedious load–deflection analysis.

References

Ahn JM and Shin SW (2007) An evaluation of ductility of high-strength reinforced concrete columns subjected to reversed cyclic loads under axial compression. *Magazine of Concrete Research* **59(1)**: 29–44.

Baczkowski BJ and Kuang JS (2008) A new approach to testing concrete coupling beams subjected to reversed cyclic loading. *Magazine of Concrete Research* **60(4)**: 301–309.

Bae S and Bayrak O (2008) Plastic hinge length of reinforced concrete columns. *ACI Structural Journal* **105(3)**: 290–300.

Bai ZZ and Au FTK (2009) Ductility of symmetrically reinforced concrete columns. *Magazine of Concrete Research* **61(5)**: 345–357.

Bai ZZ, Au FTK and Kwan AKH (2007) Complete nonlinear response of reinforced concrete beams under cyclic loading. *The Structural Design of Tall and Special Buildings* **16(2)**: 107–130.

Bayrak O and Sheikh SA (1998) Confinement reinforcement design consideration for ductile HSC columns. *Journal of Structural Engineering, ASCE* **124(9)**: 999–1010.

Bayrak O and Sheikh SA (2001) Plastic hinge analysis. *Journal of Structural Engineering, ASCE* **127(9)**: 1092–1100.

CEN (European Committee for Standardization) (2004) Eurocode 2: Design of concrete structures: Part 1-1: General rules and rules for buildings. European Committee for Standardization, Brussels.

Daniell JE, Oehlers DJ, Griffith MC, Mohamed Ali MS and Ozbakkaloglu T (2008) The softening rotation of reinforced concrete members. *Engineering Structures* **30(11)**: 3159–3166.

Haskett M, Oehlers DJ, Mohamed Ali MS and Wu C (2009) Rigid body moment–rotation mechanism for reinforced concrete beam hinges. *Engineering Structures* **31(5)**: 1032–1041.

Ho JCM (2003) *Inelastic Design of Reinforced Concrete Beams and Limited Ductile High-Strength Concrete Columns*. PhD thesis, The University of Hong Kong, Hong Kong.

Ho JCM and Pam HJ (2003a) Inelastic design of low-axially loaded high-strength reinforced concrete columns. *Engineering Structures* **25(8)**: 1083–1096.

Ho JCM and Pam HJ (2003b) Influence of transverse steel configuration on post-elastic behaviour of high-strength reinforced concrete columns. *Transactions of the Hong Kong Institution of Engineers* **10(2)**: 1–9.

Ho JCM and Pam HJ (2004) Extent of critical region and limited ductility design of high-strength reinforced concrete columns for Hong Kong practice. *Transactions of the Hong Kong Institution of Engineers* **11(3)**: 17–28.

Ho JCM, Kwan AKH and Pam HJ (2003) Theoretical analysis of post-peak flexural behaviour of normal- and high-strength concrete beams. *The Structural Design of Tall and Special Buildings* **12(2)**: 109–125.

Ho JCM, Kwan AKH and Pam HJ (2004) Minimum flexural ductility design of high-strength concrete beams. *Magazine of Concrete Research* **56(1)**: 13–22.

Hong KN, Akiyama M, Yi ST and Suzuki M (2006) Stress–strain behaviour of high-strength concrete columns confined by low-volumetric ratios rectangular ties. *Magazine of Concrete Research* **58(2)**: 101–115.

Inel M and Ozmen HB (2006) Effects of plastic hinge properties in nonlinear analysis of reinforced concrete buildings. *Engineering Structures* **28(11)**: 1494–1502.

Inel M, Aschheim MA and Pantazopoulou SJ (2007) Seismic deformation capacity indices for concrete columns: model estimates and experimental results. *Magazine of Concrete Research* **59(4)**: 297–310.

Jaafar K (2008) Shear behaviour of reinforced concrete beams with confinement near plastic hinges. *Magazine of Concrete Research* **60(9)**: 665–672.

Kim TH, Kim YJ and Shin HM (2007) Seismic performance assessment of reinforced concrete bridge columns under variable axial load. *Magazine of Concrete Research* **59(2)**: 87–96.

Kwan AKH and Au FTK (2004) Flexural strength–ductility performance of flanged beam sections cast of high-strength concrete. *The Structural Design of Tall and Special Buildings* **13(1)**: 29–43.

Kwan AKH, Ho JCM and Pam HJ (2002) Flexural strength and ductility of reinforced concrete beams. *Proceedings of the Institution of Civil Engineers, Structures and Buildings* **152(4)**: 361–369.

Kwan AKH, Au FTK and Chau SL (2004) Theoretical study on effect of confinement on flexural ductility of normal and high-strength concrete beams. *Magazine of Concrete Research* **56(5)**: 299–309.

Kwan AKH, Chau SL and Au FTK (2006) Design of high-strength concrete beams subjected to small axial load. *Magazine of Concrete Research* **58(6)**: 333–341.

Lam SSE, Wu B, Wong YL, Wang ZY, Liu ZQ and Li CS (2003) Drift capacity of rectangular reinforced concrete columns with low lateral confinement and high-axial load. *Journal of Structural Engineering, ASCE* **129(6)**: 733–742.

Lam JYK, Ho JCM and Kwan AKH (2009) Flexural ductility of high-strength concrete columns with minimal confinement. *Materials and Structures* **42(7)**: 909–921.

Li B, Park R and Tanaka H (1991) Effect of confinement on the behaviour of high strength concrete columns under seismic loading. *Proceedings of the Pacific Conference on Earthquake Engineering*, Auckland, New Zealand, November, pp. 67–78.

Marefat MS, Khanmohammadi M, Bahrani MK and Goli A (2006) Experimental assessment of reinforced concrete columns with deficient seismic details under cyclic load. *Advances in Structural Engineering* **9(3)**: 337–347.

Morley CT (2008) When plasticity? *Magazine of Concrete Research* **60(1)**: 561–568.

Pam HJ and Ho JCM (2001) Flexural strength enhancement of confined reinforced concrete columns. *Proceedings of the Institution of Civil Engineers, Structures and Buildings* **146(4)**: 363–370.

Park R and Paulay T (1975) *Reinforced Concrete Structures*. John Wiley, New York, USA.

Paultre P, Legeron F and Mongeau D (2001) Influence of concrete strength and transverse reinforcement yield strength on behaviour

of high-strength concrete columns. *ACI Structural Journal* **98(4)**: 490–501.

Sharma UK, Bhargava P and Sheikh SA (2007) Tie-confined fibre-reinforced high-strength concrete short columns. *Magazine of Concrete Research* **59(10)**: 757–769.

Sheikh SA and Yeh CC (1990) Tied concrete columns under axial load and flexure. *Journal of Structural Engineering, ASCE* **116(10)**: 2780–2800.

Sheikh SA, Shah DV and Khoury SS (1994) Confinement of high-strength concrete columns. *ACI Structural Journal* **91(1)**: 100–111.

Spence R (2008) Earthquake loss estimation for reinforced concrete buildings: some problems. *Magazine of Concrete Research* **60(9)**: 701–707.

Su RKL, Pam HJ and Lam WY (2006) Effects of shear connectors on plate-reinforced composite coupling beams of short and medium-length spans. *Journal of Constructional Steel Research* **62(1–2)**: 178–188.

Su RKL, Lam WY and Pam HJ (2009) Experimental study of plate-reinforced composite deep coupling beams. *Structural Design of Tall and Special Buildings* **18(3)**: 235–257.

Watson S and Park R (1994) Simulated seismic load tests on reinforced concrete columns. *Journal of Structural Engineering, ASCE* **120(6)**: 1825–1849.

Woods JM, Kiousis PD, Ehsani MR, Saadatmanesh H and Fritz W (2007) Bending ductility of rectangular high strength concrete columns. *Engineering Structures* **29(8)**: 1783–1790.

Wu YF, Oehlers DJ and Griffith MC (2004) Rational definition of the flexural deformation capacity of RC column sections. *Engineering Structures* **26(5)**: 641–650.

Xiao X, Guan FL and Yan S (2008) Use of ultra-high-strength bars for seismic performance of rectangular high-strength concrete frame columns. *Magazine of Concrete Research* **60(4)**: 253–259.

Youm KS, Lee YH, Choi YM, Hwang YK and Kwon TG (2007) Seismic performance of lap-spliced columns with glass FRP. *Magazine of Concrete Research* **59(3)**: 189–198.

Youssef MA and Rahman M (2007) Simplified seismic modelling of reinforced concrete flexural members. *Magazine of Concrete Research* **59(9)**: 639–649.

Discussion contributions on this paper should reach the editor by 1 February 2011